The Cyclization Mechanism of Cyclodextrin Glycosyltransferase (CGTase) as Revealed by a γ-Cyclodextrin-CGTase Complex at 1.8-Å Resolution

Uitdehaag, Joost C.M.; Kalk, Kor H.; Veen, Bart A. van der; Dijkhuizen, Lubbert; Dijkstra, Bauke W.

Link to publication in University of Groningen/UMCG research database

The Cyclization Mechanism of Cyclodextrin Glycosyltransferase (CGTase) as Revealed by a γ-Cyclodextrin-CGTase Complex at 1.8-Å Resolution*

Joost C. M. Uitdehaag‡, Kor H. Kalk‡, Bart A. van der Veen§, Lubbert Dijkhuizen§, and Bauke W. Dijkstra‡¶

From the ‡BIOSON Research Institute and Laboratory of Biophysical Chemistry, Groningen Biomolecular Sciences and Biotechnology Institute (GBB), University of Groningen, Nijenborgh 4, 9747AG Groningen, the Netherlands and §Department of Microbiology, GBB Institute, University of Groningen, Kerklaan 30, 9751 NN Haren, the Netherlands

The enzyme cyclodextrin glycosyltransferase is closely related to α-amylases but has the unique ability to produce cyclodextrins (circular α(1→4)-linked glucoses) from starch. To characterize this specificity we determined a 1.8-Å structure of an E257Q/D229N mutant cyclodextrin glycosyltransferase in complex with its product γ-cyclodextrin, which reveals for the first time how cyclodextrin is competently bound. Across subsites −2, −1, and +1, the cyclodextrin ring binds in a twisted mode similar to linear sugars, giving rise to deformation of its circular symmetry. At subsites −3 and +2, the cyclodextrin binds in a manner different from linear sugars. Sequence comparisons and site-directed mutagenesis experiments support the conclusion that subsites −3 and +2 confer the cyclization activity in addition to subsite −6 and Tyr-195. On this basis, a role of the individual residues during the cyclization reaction cycle is proposed.

The α-amylase family, or glycosyl hydrolase family 13 (1), is an extensively studied enzyme family (2, 3) that comprises many enzymes used in industrial starch processing (4, 5). All family 13 enzymes use a so-called α-retaining double displacement mechanism (6, 7) to produce a surprisingly large variety of oligoglucoside products (2). As an illustration, α-amylases hydrolyze α(1→4) glycosidic bonds to produce shorter α(1→4)-linked oligosaccharides. On the other hand, that same α(1→4) glycosidic bond is cleaved by isoamylase (8) and malto-oligosyl-trehalose synthase (9) to produce α(1→6) and α(1→1) glycosidic linkages, respectively. For an overview of the α-amylase family, see the ALAMY data base (Š. Janeček) on the Internet.

An especially interesting and unique family 13 enzyme is cyclodextrin glycosyltransferase (CGTase).[1] CGTase forms circular α(1→4)-linked oligoglucosides called cyclodextrins from linear α(1→4)-linked glucans via an intramolecular transglycosylation reaction known as cyclization (see Fig. 1). In addition, CGTase can perform hydrolysis (very poorly) and disproportionation reactions by using water or a free oligosaccharide as respective acceptors. Its ability to perform cyclization has led to the application of CGTases in the industrial production of cyclodextrins (4).

CGTases are typically 75-kDa proteins consisting of 5 domains (A-E) (10, 11). Domains A and B constitute the catalytic domains, whereas C and E are specialized in binding to raw starch granules (11, 12). Domain D has no known function. The active site of *Bacillus circulans* strain 251 CGTase was shown to comprise at least nine sugar binding subsites (13), labeled −7 to +2. Bond cleavage occurs between subsites −1 and +1 (see Fig. 1), resulting in an intermediate that is covalently linked to Asp-229 at subsite −1 (7). During cyclization, CGTase circularizes the linear chain of this intermediate (7) such that the nonreducing end glucose residue moves from subsite −7 into subsite +1. There it is used as the acceptor sugar and becomes covalently linked to the C1 atom of the sugar at subsite −1 (see Fig. 1). We denote this sugar transfer step circularization to distinguish it as a subprocess of cyclization. Astonishingly, circularization requires a 23 Å-movement of the linear chain end (13). Kinetic data suggest that this is the rate-limiting step in the cyclization reaction.[2]

The mechanism of cyclization has been extensively studied to gain insight into the factors that determine the substrate specificity of the enzyme and the reaction type specificity and to improve CGTase for industrial applications. Site-directed mutagenesis studies covering almost all sugar binding subsites show that specific residues at subsites +2, −3, and −6 contribute to cyclization (reviewed in Table I, see "Discussion"). Of particular importance is the centrally located residue Tyr-195, as was demonstrated in at least 6 different CGTases (Table I). To understand how these residues confer cyclization activity, structural information about the individual stages of the reaction cycle is essential.

Crystallographic investigations have already revealed how a maltononaose substrate and a covalent maltotriosyl intermediate bind in the active site of CGTase (7, 13). (Fig. 1). However, it is unknown how CGTase binds a cyclodextrin product. A structure of a CGTase-β-cyclodextrin derivative complex has been determined, but this shows a cyclodextrin that has already partly departed from the catalytic site (14). Here we present the 1.8-Å structure of a γ-cyclodextrin that is competently bound in the active site of *B. circulans* strain 251 E257Q/

TABLE I
The function of residues in CGTase sugar binding subsites

Residue No.[a]	Residue in α-amylase (38)[b]	Residue in CGTase sequences[c]	Function in CGTase[d]
Subsite +2			Acceptor
183	Tyr	**Phe**	Cyclization (30)
232	Lys	Lys	Disproportionation[e]
259	Leu	**Phe/Tyr**	Cyclization and disproportionation (30, 46)
Subsite +1			Acceptor
194	Leu	Leu	Cyclization (47)
230	Thr[f]	Ala[f]	—
233	His	His	General activity (36, 48)
Subsite −1			Catalytic
The architecture of subsite −1 is conserved in the entire α-amylase family (3, 7)			
Subsite −2			Donor
98	His	His	General activity (48)
101	Trp	Trp	—
375	Arg	Arg	—
Subsite −3			Donor
89	—	Tyr/Asp/Ser	Cyclization and specificity (44, 49)
94	—	Asn/Ser/-	Cyclization and specificity (49)
371	Asp	Asp	Cyclization[e] (17)
196	—	**Asp**	Cyclization[e] (17)
47	—	Arg/Lys/His	Cyclization[e]
Subsites −4 and −5			No side chain contacts
Subsite −6			Donor
167	—	**Tyr**	—
179	—	**Gly**	—
180	—	**Gly**	—
193	—	**Asn**	Cyclization[e]
Subsite −7			Donor
145	—	Ser/Met/Leu/..	Specificity[e] (47)
146	—	Glu/Ser/Arg/..	Specificity (44, 47)
147	—	Thr/Asp	Specificity (47)
Central			
195	Gly	**Tyr/Phe**	Cyclization (30, 37, 44, 46, 47, 50)

[a] Residues delimiting the subsite surface with their side chains.

[b] Identification based on a superposition of 3-dimensional structures. Dashes denote the absence of the corresponding residues in α-amylases.

[c] On the basis of 20 CGTase sequences which were downloaded using Entrez. Boldface indicates that a residue is conserved in CGTase but not in α-amylases. Amino acid variations at a position are separated by a slash, with the most frequently occurring type given first, with a dash denoting a deletion. If a variation comprises more than three amino acid types, two dots are given in fourth position.

[d] The residue function is derived from the relatively most decreased type of activity after site-directed mutagenesis, and specificity refers to the cyclodextrin size ratio produced.

[e] Function based on unpublished results.

[f] Mammalian α-amylases have a conserved Ala at position 230; therefore Ala 230 is not indicated as typical for CGTase.

D229N CGTase. Our data provide for the first time detailed insights in the mechanisms that are employed by CGTase to perform the cyclization reaction.

EXPERIMENTAL PROCEDURES

Soaking Procedure—Crystals of *B. circulans* strain 251 CGTase were grown from 60% (v/v) 2-methyl-2,4-pentanediol (MPD), 100 mM HEPES, pH 7.55, and 5.0% (w/v) maltose (11). In the past, various x-ray structures of CGTase-oligosaccharide complexes have been obtained after soaking crystals in a mother liquor where the maltose had been replaced by another sugar or inhibitor (13, 15, 16). However, when cyclodextrins are used for soaking, they are digested to small linear oligosaccharides (15). To prevent this, we used crystals of the marginally active E257Q/D229N CGTase (15) equilibrated at pH 10.3. One of these crystals was soaked for 30 min in a solution containing 60% MPD and 100 mM CAPS buffer at pH 10.3 saturated with γ-cyclodextrin. Thereafter it was frozen under a cold nitrogen stream (120 K) for data collection using the soaking solution as cryo-protectant.

Data Collection and Refinement—Data to 1.78 Å were collected at beamline X11 of the EMBL outstation at DESY, Hamburg. The data were processed and refined using standard crystallographic techniques (17) involving DENZO (18), O (19), TNT (20), and ARP (21). Normal and OMIT (22) electron density maps were calculated with the BIOMOL package, applying the SIGMAA procedure (23). As a starting model, we used the 2.2-Å structure of unliganded wild type CGTase at pH 7.55 and 120 K (15). From the initial electron density map it was obvious that three γ-cyclodextrins were bound, one in the active site and two at the raw starch binding sites in the E-domain (MBS1 and MBS2 (11)). At MBS3 in the C-domain a maltose was observed, as in other CGTase structures (11). The γ-cyclodextrins were built into their electron density and refined using the stereochemistry from their crystal structure (24).

Halfway through refinement we observed density for a MPD molecule near residues Pro-379 and Arg-377, which was included in the model using stereochemical parameters from the hetero compounds data base (G. Kleywegt, Uppsala University, Uppsala, Sweden). One water molecule refined to a suspiciously low B-factor of 2.2 Å^2. It had an $F_o − F_c$ OMIT electron density peak of 17 times the standard deviation and was surrounded by the atoms Ala-315 O at 2.3 Å and Asp-577 Oδ1 (in a new orientation) at 2.7 Å as well as 3 water molecules at a 2.4-Å distance. The peak height and ligation suggested the presence of a third Ca^{2+} binding site in addition to the two Ca^{2+} sites observed earlier (11). It is located far from the active site, at the interface of the A and D domains. Inspection of other data sets revealed a similar peak in a 1.5-Å-unliganded CGTase structure at pH 10.3[3] but not in any other structure determined at a lower pH. Therefore, most likely this third Ca^{2+} site is an artifact of the high pH used, with little relevance for the activity of CGTase at optimal pH (pH 5.5).

In the final stage of the refinement the orientations of His, Gln, and Asn residues were determined by optimization of their hydrogen-bonding networks (25). In addition, the Asn and Gln orientations were verified by the difference in atomic B-factors of their Oδ/ε and Nδ/ε atoms (with the program ACT (26)). The stereochemistry of all amino acids was verified with PROCHECK (27) and WHATCHECK (25). The final electron density for the γ-cyclodextrin bound in the active site is shown in Fig. 2. Data and refinement statistics are given in Table II.

Verification of the Results—To exclude artifacts arising from the pH, mutations, or temperature, we first compared the structures of unliganded E257Q/D229N CGTase at 120 K, pH 10.3,[3] with unliganded wild type CGTase at 120 K, pH 7.6 (15), and 293 K, pH 7.6 (11). No significant differences were observed. Second, we restricted functional comparisons to CGTase structures that were determined under identi-

---

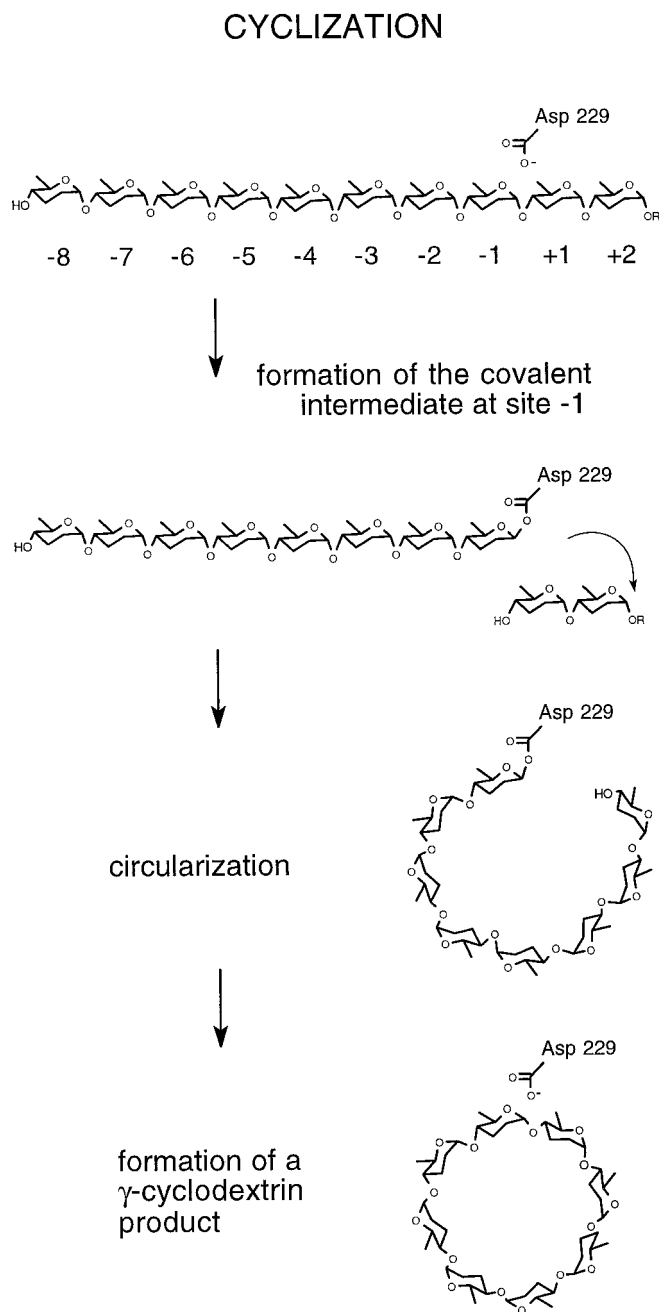[3] J. C. M. Uitdehaag, unpublished result.

CYCLIZATION

FIG. 1. **Schematic representation of the cyclization reaction catalyzed by CGTase.** After the first, bond-cleavage step, a covalent intermediate is formed (7). In the second step the linear chain assumes a cyclic conformation, which is denoted as the circularization step. In the third step, a new glycosidic bond is formed with the 4-OH group of the glucose unit in subsite +1. The catalytic residues involved in bond cleavage are Asp-229 and Glu-257 (16) (the latter is not shown). The formation of γ-cyclodextrin (eight glucose units) is illustrated, but CG-Tase also produces the smaller α- and β-cyclodextrins (six and seven glucoses, respectively) and larger cyclodextrins (45).

cal experimental conditions, which warrants that all observed differences are ligand-induced.

RESULTS

Binding of the γ-Cyclodextrin in the Catalytic Site of CG-Tase—In the CGTase-cyclodextrin complex, two γ-cyclodextrin molecules are bound at the maltose binding sites (MBS) MBS1 and MBS2 in the E domain, and one is bound in the active site. The electron density clearly shows that the cyclic symmetry of the latter CD is spectacularly deformed (Figs. 2 and 3) by the catalytic site architecture that has forced the +1 glucose out of

the ring structure. As a result, the torsion angles of the scissile bond have acquired a characteristic twist (16). This brings the glucoses at subsites −1 and +1 close to the catalytic residues and makes them superimpose well with other CGTase and α-amylase ligand complexes (16, 28, 29). This assures us that the γ-cyclodextrin is bound in a catalytically competent fashion, in contrast to the earlier CGTase-β-cyclodextrin complex (14).

Comparison of γ-Cyclodextrin and Maltononaose Substrate Binding Modes—To gain insight into the cyclization mechanism, the binding mode of γ-cyclodextrin was compared with that of a linear maltononaose substrate bound from subsites −7 to +2 (7). Both structures were determined under identical experimental conditions. A superposition is shown in Fig. 3. At subsites −2, −1, and +1, both ligands are bound in a nearly identical fashion. Both show the "twist" discussed above and also distortion of the glucose ring at subsite −1 toward transition state planarity (7). In contrast, at subsites +2 and −3, γ-cyclodextrin is bound differently from maltononaose. At subsite −3 the cyclodextrin glucose has a position more toward the central residue Tyr-195 (see Fig. 4, *A* and *C*), and at subsite +2 the cyclodextrin glucose is bound upside down compared with that in maltononaose (see Fig. 4*B*). The three remaining glucose moieties of the γ-cyclodextrin molecule (labeled −4c, +3c, and +4c) are not bound by any amino acids. The cyclodextrin molecule rests on top of Tyr-195, which does not protrude into the hydrophobic interior of cyclodextrin, in contrast to previous hypotheses (30). An overview of all interactions is presented in Table III and Fig. 5.

Geometry of the CGTase γ-Cyclodextrin and Maltononaose Ligands—The γ-cyclodextrin and maltononaose ligands have favorable bond lengths and angles in all sugars (24). In addition, all glucoses assume a favorable $^{4}C_{1}$ chair conformation, except for those that bind in subsite −1 (7). However, the internal hydrogen bond network between the glucose OH-2 and OH-3 groups, which is observed in both free cyclodextrins (24, 31) and free starch (32), is broken between subsites −1/+1 and +1/+2 (see Table III and Fig. 5). In the CGTase-maltononaose complex (7), the OH-2/OH-3 network is in addition broken between subsites −2/−3, −4/−5, and −5/−6 but not between +1/+2 (as judged from an O2-O3 distance >3.3 Å, see Table III and Fig. 5). That these hydrogen bonds are usually present even when malto-oligosaccharides are in aqueous solution (31, 33) suggests that CGTase distorts the conformation of maltononaose energetically more than that of γ-cyclodextrin.

Flexibility in the CGTase γ-Cyclodextrin and Maltononaose Ligands—Sugar flexibility can give important information on binding interactions. It can be judged from the experimentally determined atomic B-factors. The γ-cyclodextrin and maltononaose complexes were refined using similar protocols, making their B-factors comparable. In the γ-cyclodextrin complex (average B-factor, 16 Å^{2}), the glucose rings are relatively fixed in subsites −2 (21 Å^{2}), −1 (18 Å^{2}), and +1 (16 Å^{2}) and are increasingly flexible in subsites −3 (28 Å^{2}) and +2 (24 Å^{2}) and even more in −4c (37 Å^{2}), +4c (37 Å^{2}), and +3c (33 Å^{2}). In contrast, the maltononaose (average B-factor, 12 Å^{2}) is fixed both at subsites −2 (14 Å^{2}), −1 (11 Å^{2}), +1 (16 Å^{2}), and at subsites −6 (17 Å^{2}) and −7 (16 Å^{2}, involved in crystal contacts). Flexibility is increased at the reducing end +2 (30 Å^{2}) and at subsites −3 (24 Å^{2}), −4 (24 Å^{2}), and −5 (22 Å^{2}). This confirms that subsites −4 and −5 make weak interactions (Table III) and that subsites −3 and +2 can bind multiple sugar conformations (see below). In contrast, subsites −2, −1, and +1, supporting only one sugar binding mode, bind sugars rigidly. Interestingly, the glucose in the catalytic site −1 is more rigid in the maltononaose substrate complex (below average B) than
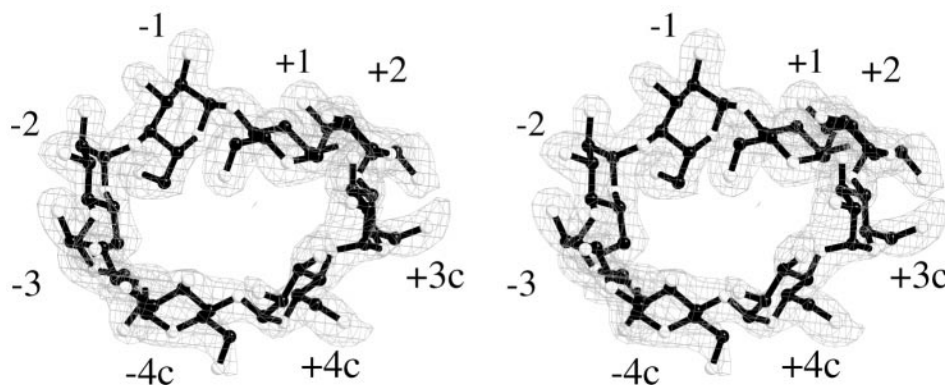
FIG. 2. **Stereo picture of the final σ_A-weighted $2F_o - F_c$ electron density that defines the γ-cyclodextrin bound in the CGTase active site.** The density was contoured at 1 unit S.D. (1σ). The labels indicate subsite nomenclature.

TABLE II

Data collection statistics and quality of the B. circulans strain 251 E257Q/D229N CGTase-γ-cyclodextrin complex

Temperature, pH	120 K, pH 10.3
X-ray source	EMBL Hamburg, beamline X11
Space group	$P2_12_12_1$
Cell axes a, b, c (Å)	117.7, 109.0, 65.3
Resolution range	30.0–1.78 Å
No. of unique reflections	78,716
Completeness	97.3%
$R_{merge}{}^a$	6.2%
Average signal to noise ratio (I/σ)	18.9
Completeness in the last resolution shell	71.0% (1.81–1.78 Å)
$R_{merge}{}^a$ in the last resolution shell	28.5% (1.81–1.78 Å)
I/σ in the last resolution shell	3.6 (1.81–1.78 Å)
Refinement statistics	
No. of amino acids/Ca^{2+}/MPD/waters	686 (all)/3/1/639
Active site ligand	γ-Cyclodextrin
Maltose binding site 1 (11)	γ-Cyclodextrin
Maltose binding site 2 (11)	γ-Cyclodextrin
Maltose binding site 3 (11)	Maltose
Average B-factor	18.8 Å^2
Final R factor^b (8.0–1.78 Å)	22.0% (solvent-corrected)
Final free R factor^c (8.0–1.78 Å)	25.8% (solvent-corrected)
Average coordinate error (σ_A) (23)	0.18 Å
Root mean square deviation from ideal geometry	
Bond lengths (Å)	0.006 Å
Bond angles (degree)	0.735 °
Torsion angles	17.0 °
Trigonal planes	0.007 Å
Planar groups	0.011 Å
van der Waals contacts (Å)	0.011 Å
B-factor correlations (Å^2)	1.518 Å^2

^{a} $R_{merge} = \Sigma_h \Sigma_i |I(h) - I_i(h)|/\Sigma_h \Sigma_i I_{i(h)}$, where reflection h has intensity $I_i(h)$ on occurrence i and mean intensity $I(h)$.

^{b} R factor $= \Sigma_h |F_o - F_c|/\Sigma_h F_o$, where F_o and F_c are the observed and calculated structure factor amplitudes of reflection h, respectively.

^{c} The free R factor is calculated as the R factor, using F_o that were excluded from the refinement (5% of the data).

in the γ-cyclodextrin complex (above average B).

Subsite +2 Binds Two Different Sugar Conformations—At subsite +2, the γ-cyclodextrin and maltononaose ligands bind in very different conformations, which are both supported by good binding interactions (Table III, Figs. 4*B* and 5). In maltononaose, the glucose at subsite +2 is positioned with its A face (34) toward Phe-183 in an orientation more parallel to Phe-183 than to Phe-259 (*gray ring* in Fig. 4*B*). This indicates that the best hydrophobic stacking interactions (34) are made to Phe-183. Furthermore, the glucose O6 atom is pointing toward Tyr-195, while the sugar O3 atom forms a good 2.8-Å hydrogen bond to Lys-232 (Fig. 4*B*).

In contrast, the γ-cyclodextrin complex has the subsite +2 glucose residue bound with the other side up. Now the sugar

ring A face is oriented parallel and close to Phe-259, indicating good stacking interactions with this residue (Fig. 4*B*). Interactions with Phe-183 are limited. The cyclodextrin glucose O6 atom is at a 3.3-Å distance from the Lys-232 Nζ atom, but the geometry is not compatible with the presence of a hydrogen bond (Fig. 4*B*). In summary, at subsite +2, residues Lys-232 and Phe-183 seem to prefer binding to linear substrate, whereas Phe-259 interacts best with cyclodextrin.

Subsite −3 Binds Two Different Sugar Conformations—Subsite −3 is also sufficiently promiscuous to provide good contacts with both maltononaose and γ-cyclodextrin (see Figs. 4*A* and 5). The binding of maltononaose at subsite −3 is characterized by a 2.7-Å hydrogen bond between the Asp-371 Oδ2 atom and the glucose OH-2 group and by a hydrogen bond between the Asp-196 Oδ1 atom and the substrate OH-6 group. The Asp-196 Oδ2 atom forms a hydrogen bond with the Tyr-89 Oη atom (Fig. 4*A*). This small hydrogen-bonding network is stabilized by the hydrophobic environment provided by Tyr-89, Pro-43, Leu-197, Trp-101, Ile-87, Phe-151 and the glucose at subsite −4.

In the cyclodextrin complex, the glucose at subsite −3 is oriented more toward Tyr-195. Residue Asp-196 does not contact the substrate directly but via a water molecule that binds to the glucose atoms O6 (2.7 Å) and O5 (3.1 Å) (Fig. 4*A*). As in the maltononaose structure, a contact between Asp-371 Oδ2 and the glucose OH-2 group is observed, but Asp-371 is displaced by 0.6 Å to accommodate the new binding mode (Fig. 4*A*). In addition, Arg-47 binds to the O2 and O3 glucose atoms of the cyclodextrin (Fig. 4*A*). This is the first time that Arg-47 is implicated in direct sugar binding. To make this binding contact, the side chain of Arg-47 has assumed a new conformation compared with unliganded wild type CGTase (15). Thus, at subsite −3, Arg-47 specifically binds to cyclodextrin, and residue Asp-196 interacts better with a long linear sugar, whereas Asp-371 can support both binding modes.

Ligand-induced Changes in the Main-chain Conformation of CGTase—The main chain of the γ-cyclodextrin-complexed CG-Tase superimposes very well on that of unliganded CGTase (15) (root mean square deviation, 0.16 Å for 686 Cα atoms). The only exceptions occur in the loops comprising residues 324–334 (involved in catalysis around subsite −1 (7)) and 144–151 (involved in altered crystal contacts). Thus, to bind a γ-cyclodextrin, CGTase does not need to adjust its main-chain conformation.

The situation is different when maltononaose-liganded CG-Tase is compared with unliganded CGTase (root mean square deviation, 0.30 Å for 686 Cα atoms). The relative orientation of the A and E domains has changed slightly, and the sugar binding cleft has narrowed. As in the γ-CD complex, the loops 144–151 and 324–334 have a slightly different conformation. In addition, the loop 190–199, which contains the important

FIG. 3. **Stereo picture indicating the maltononaose (7) (*gray*) and γ-cyclodextrin (*black*) conformation in the CGTase active site.** The *white* Cα backbone has the conformation observed in the γ-cyclodextrin complex. The backbone conformations of the loops 87–93 144–151, 175–182, and 190–199 in the maltononaose complex are indicated in *gray*.
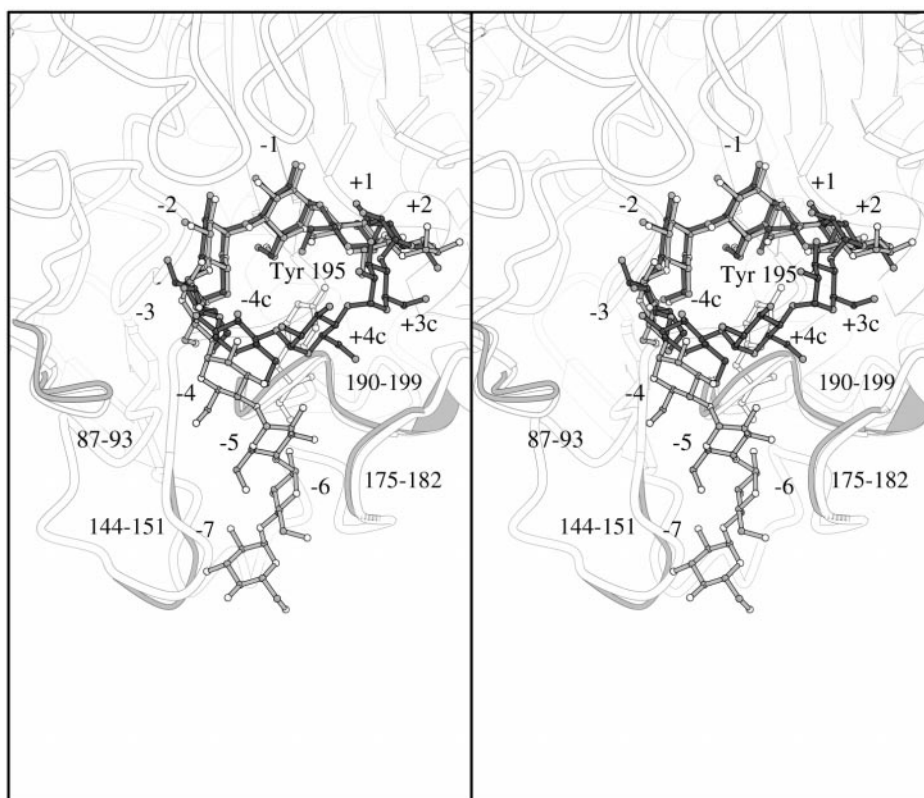
residue Tyr-195, shows a maximal shift of 0.5 Å (see Figs. 3 and 4C). Residues 190 and 199 at both ends of this loop are Ca^{2+} ion ligands (see Fig. 4C). Another loop, comprising residues 87–93, has been displaced up to ~1.3 Å. This loop forms one side of subsite −3 and shows significantly better electron density in the maltononaose complex than in any other *B. circulans* strain 251 CGTase complex. Its reorientation might be caused by sugar binding at subsite −3, since superposition of maltononaose on the unliganded CGTase conformation reveals weak van der Waals repulsions between the glucose C5 and O6 atoms and the Tyr-89 aromatic ring (see Fig. 4A).

A final interesting loop is 175–182, which forms one side of subsites −5 and −6 (Fig. 3). It is displaced by ~0.7 Å, bringing the main-chain atoms of residues Gly-179 and Gly-180 closer to the bound glucose at subsite −6 (Fig. 3) (~4 Å). All these loops are intimately connected through various interactions. Thus, in conclusion, maltononaose binding, but not γ-cyclodextrin binding, causes a clear induced-fit effect in the active site of CGTase.

Ligand-induced Changes in the Conformation of Tyr-195— Together with the main-chain plasticity, the x-ray structures reveal a large conformational flexibility for Tyr-195 (Fig. 4). In the γ-cyclodextrin-liganded CGTase, the Tyr-195 side chain points toward Phe-183. The Tyr-195 Oη atom takes part in a three-centered hydrogen bond with the OH-6 and O5 groups of the sugar at subsite +1 (35) (Fig. 4B). However, in the maltononaose complex, Tyr-195 has rotated and shifted 2.6 Å toward subsite −3 (Fig. 4, B and C). The Tyr-195 Oη atom now binds to the maltononaose OH-6 group in subsite +1 only.

This reorientation of Tyr-195 and the shift of loop 190–199 might be caused by a strong steric repulsion at subsite −6. If maltononaose is superimposed on the unliganded CGTase structure, the backbone carbonyl oxygen of Tyr-195 and the substrate O2 atom at subsite −6 are at only 2.0 Å distance (Fig. 4C). In addition, the Tyr-195 conformation observed in the maltononaose complex would clash in a ~2.0-Å van der Waals contact with a γ-cyclodextrin ligand at subsite −3 (Fig. 4C).

This implies that Tyr-195, after being reoriented by maltononaose binding at subsite −6, is involved in keeping the sugar at subsite −3 in its observed position.

Ligand-dependent Conformations of Asn-139 and His-140 at Subsite −1—Although the glucoses of maltononaose and γ-cyclodextrin in the catalytic site (−1) occupy similar positions, there is an interesting difference in the conformations of the catalytic site residues His-140 and Asn-139. In cyclodextrin-liganded CGTase, the His-140 Nδ atom binds to the carbonyl oxygen of Tyr-100, whereas the His-140 Nε atom forms a hydrogen bond to the Asn-139 Nδ atom (*purple* in Fig. 4C). The Asn-139 Oδ atom acts as a Ca^{2+} ligand. This His-140 conformation prevents it from binding the −1 glucose residue of γ-CD, which is unexpected, because mutagenesis experiments indicate a role for His-140 in sugar binding and transition state stabilization (3, 36). Nevertheless, this His-140–Asn-139 conformation is also observed in unliganded wild type CGTase (15) as well as in inhibitor complexes of CGTase (16) and α-amylases (28, 29).

The situation is different in the maltononaose substrate complex. Here the side chain of Asn-139 has clearly rotated away from Ca^{2+}, thereby disrupting the hydrogen bond to His-140 (*gray* in Fig. 4C). In addition, the electron density and hydrogen bond network suggest that the imizadole ring of His-140 is flipped. This enables the 140 Nδ atom to bind the Thr-141 carbonyl oxygen and the 140 Nε atom to bind the maltononaose OH-6 group at subsite −1 (Figs. 4C and 5). This hydrogen bond to the substrate agrees better with the role of His-140 as found from mutagenesis studies (3, 36). It suggests that in the maltononaose complex, His-140 is optimally positioned to contribute to catalysis (7).

DISCUSSION

γ-Cyclodextrin Binds Because Its Degradation Is Sterically Blocked—To elucidate the atomic basis of the CGTase cyclization reaction, we have determined the first structure of a CG-Tase with a cyclodextrin product bound competently in its
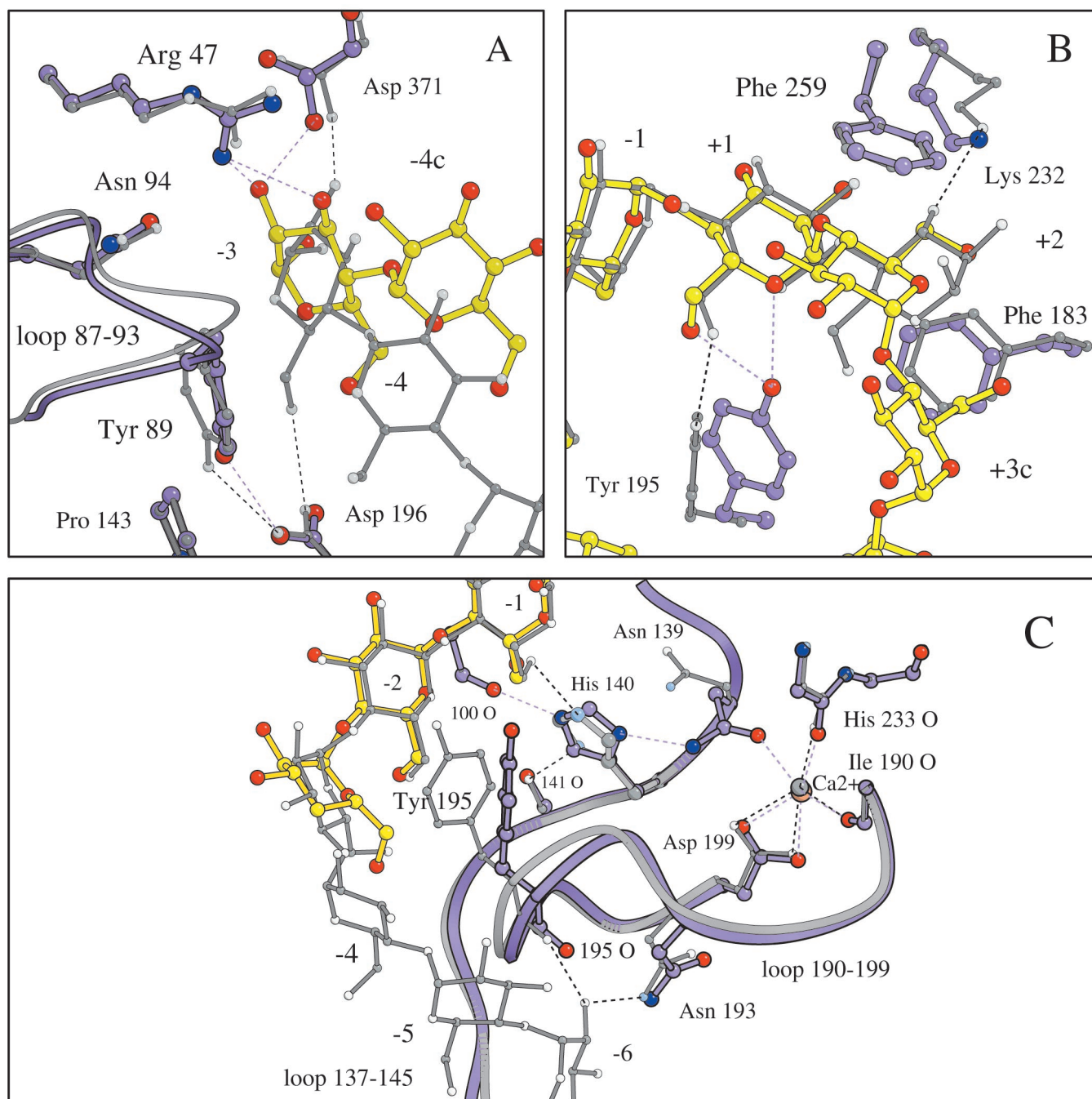
FIG. 4. **Close-ups of the γ-cyclodextrin structure (*yellow* and *red*, with corresponding amino acids in *purple*) superimposed on the maltononaose structure (7) (*gray* and *white*).** *A*, detail of subsite −3. The conformation of Arg-47 in both structures differs from wild type, unliganded CGTase (not shown). *B*, detail of subsite +2; for explanation see text. *C*, rearrangements around His-140 and the loop 190–199. For clarity the cyclodextrin is only drawn at subsites −1 to −3.

active site. This was achieved by using γ-cyclodextrin (eight glucoses) for soaking instead of α- or β-cyclodextrin (six and seven glucoses, respectively). These latter CDs are degraded by coupling reactions in which the products can bind stably inside the crystal (7, 15). However, a coupling reaction with γ-cyclodextrin would presumably lead to an intermediate that binds at subsite −8, which is blocked by a crystal contact, thereby forming a kinetic barrier to γ-cyclodextrin degradation.

The 1.8-Å CGTase-γ-cyclodextrin complex was compared with the 2.1-Å CGTase-maltononaose complex (representing a bound linear substrate (7)). Both structures were determined under experimentally identical conditions. These ligands are not stable states of the same cyclization cycle (γ-CD formation

requires a linear substrate reaching subsite −8). Moreover, *B. circulans* strain 251 CGTase forms β-CD in preference to γ-CD (37). However, cyclization is largely independent of cyclodextrin size, since many amino acids that are typical for CGTase are conserved irrespective of product specificity (see below). Therefore, comparison of both structures can give useful insight into the mechanism of cyclization.

Subsites −6, −3, and +2 Contain the Residues Involved in Cyclization—To identify amino acids involved in cyclization, we studied their degree of evolutionary conservation in the active site (Table I). First, some residues are present in all CGTase sequences as well as in *Aspergillus oryzae* α-amylase (which is the α-amylase with known structure (38) that is most homolo-

TABLE III
Interactions between substrate, product, and CGTase

For an overview of the subsites see Figs. 3 and 5. WM is shorthand for water-mediated. NA indicates a nonappropriate subsite label. — indicates the absence of an interaction.

Atoms offering contacts	Distance (Å) and the glucose atom making the contact	
	Maltononaose	γ-Cyclodextrin
Subsite +4c	NA	
Glucose atom O2 at +3c		2.8 O3
Subsite +3c	NA	
Glucose atom O2 at +2		2.7 O3
Subsite +2		
Phe-183 ring	Stacking at ~4.5	—
Lys-232 Nζ	2.8 O3	3.3 O6
Phe-259 ring	Stacking at ~4.0	Stacking at ~3.7
Glucose atom O2 at +1	2.8 O3	—
Subsite +1, −1 and −2		
Binding modes identical to earlier reports,[a] with the addition of:		
−1 His-140 Nε	3.0 O6	—
+1 Tyr-195 Oη	2.7 O6	2.8 O6 and 2.9 O5
−2 Trp-101 Nε	3.0 O6	2.8 O6
Subsite −3		
Asp-196 Oδ1	2.9 O6	WM to O6 and O5
Asp-371 Oδ2	2.7 O2	2.9 O2
Arg-47 Nη1	—	2.9 O2 and 3.1 O3
Glucose atom O3 at −2	—	3.3 O2
Subsite −4[b] or subsite −4c		
Glucose atom O3 at −3	3.0 O2	2.7 O2
Glucose atom O2 at Next site (−5 or +4c)	3.4 O3	3.1 O3
Subsite −5[b]	—	NA
Subsite −6		NA
Asn-193 Nδ	3.1 O2	
Tyr-195 O	2.7 O2	
Asp-196 O/Ala-144 O	WM to O3	
Gly-179 N/Tyr-167 Oη	WM to O3	
Gly-180 N	WM to O5 and O6	
Glucose atom O3 at −5	—	
Subsite −7		NA
Ser-145 Oγ	2.7 O3	
Ser-146 N	3.1 O2	
Asp-147 N	2.9 O3	
Asp-147 Oδ1	2.9 O4	
Ala-144 O	WM to O2	
Symmetry related Gln-491 O	2.7 O6	
Symmetry related Tyr-456 Oη	2.8 O6	
Glucose atom O3 at −6	3.3 O2	

[a] For earlier reports see Refs. 7, 13, 15–17.
[b] In an earlier report (13) water-mediated contacts were observed at these subsites.

gous to CGTase). These residues are predominantly located at subsites −2, −1, and +1 and are most likely involved in the catalysis of the bond cleavage reaction (7). Secondly, among the CGTases, some amino acid positions appear to be highly variant, especially at subsite −7 (Table I). These residues are probably not essential for cyclization but may influence the cyclodextrin product size specificity (13). All other residues, the third class, are those typical for CGTase (bold in Table I) and, therefore, are potentially involved in cyclization. They are mostly located at subsites −6, −3, and +2 and also include Tyr-195. Site-directed mutagenesis studies of CGTases, of which an overview is given in Table I, corroborate this view that subsites −6, −3, +2, and Tyr-195 are important for cyclization.

Subsite −6 Selects an Oligosaccharide of Sufficient Length for Cyclization—The first step in cyclization is substrate binding (Fig. 1). At this stage, binding of a sufficiently long oligosaccharide for cyclodextrin formation requires occupation of at least subsites −1 to −6 (leading to α-cyclodextrin). Thus, the

low affinity of subsites −4 and −5 could function to prevent binding of too short oligosaccharides. At subsite −6, the interactions of substrate with Asn-193 and Tyr-167, residues typical for CGTase, and many backbone atoms are strongly conserved (Tables I and III and Fig. 5). Two other CGTase-typical residues at subsite −6, Gly-179, and Gly-180, have no side chains, since these would sterically block substrate binding. This conservation of subsite −6 confirms its importance for the selective binding of long oligosaccharide chains.

Subsite −6 May Activate Catalysis at Subsite −1—Kinetic studies confirm an increased affinity (K_m) for linear substrates that bind at (and beyond) subsite −6. However, they also suggest that longer sugar chains have a higher k_{cat} for disproportionation and, thus, are processed more rapidly (39–41). This could further limit unwanted hydrolysis and disproportionation reactions of small oligosaccharide chains in CGTase. Our x-ray studies suggest that His-140 is involved in such an induced-fit mechanism, since it is specifically activated by binding of maltononaose.

Most likely, the trigger for His-140 activation occurs when substrate binds at subsite −6 and "pushes" away the carbonyl oxygen of Tyr-195. The subsequent reorientation of Tyr-195 and the loop 190–199 has two effects. First, it changes the ligation of the nearby Ca^{2+} ion, which could stimulate reorientation of Asn-139 (Fig. 4C). Second, Tyr-195 forces the glucose at subsite −3 into its "maltononaose" position, resulting in a rigidification of the amino acids and sugars at subsites −3 to −1 (as judged by their low atomic B-factors). Both effects provide a suitable environment for His-140 to assume its optimal orientation for catalysis.

Internal Hydrogen Bonds Promote the Cyclodextrin Binding Mode—After bond cleavage, the next step in cyclization is circularization (Fig. 1). This is intrinsically an energetically unfavorable, "uphill" process, because cyclodextrins have an unfavorable enthalpy of formation (42) and because during circularization the deformed cyclodextrin ring symmetry has to be enforced. An important contribution to circularization could come from the hydrogen bond network between the OH-2 and OH-3 groups of adjacent glucoses, which is formed in the γ-cyclodextrin complex but not in the maltononaose complex (Table III, Fig. 5B). Completion of this OH-2/OH-3 hydrogen network in the maltononaose structure could be a driving force for the displacement of the nonreducing end toward the acceptor binding sites, as would be necessary in the early stages of circularization.

Tyr-195 Stabilizes an Intermediary Stage in Circularization—Site-directed mutagenesis experiments indicate that Tyr-195 is very important for cyclization, especially its aromatic moiety (Table I) (37). However, the x-ray structures show only hydrogen bond interactions between Tyr-195 and maltononaose or γ-cyclodextrin (Table III and Fig. 5). This suggests that the aromatic ring of Tyr-195 has a role during circularization. From the x-ray structures it appears that in the maltononaose complex Tyr-195 exposes, together with Phe-183, exposes a hydrophobic surface (Fig. 4B). This could function as "greasy slide" (14, 43) to facilitate movement of the sugar chain end during circularization. Interestingly, when the glucose at subsite −3 assumes a γ-cyclodextrin-like conformation, it sterically clashes with this conformation of Tyr-195, causing the dismantling of the greasy slide in the final stages of circularization.

Subsite −3 Catalyzes the Transition from Linear to Circular Sugar Chains—During circularization, the sugar at subsite −3 has to change from a maltononaose binding mode, stabilized by Asp-196 and Asp-371, into a γ-cyclodextrin binding mode, stabilized by Arg-47 and Asp-371 (Fig. 4A). All these residues are
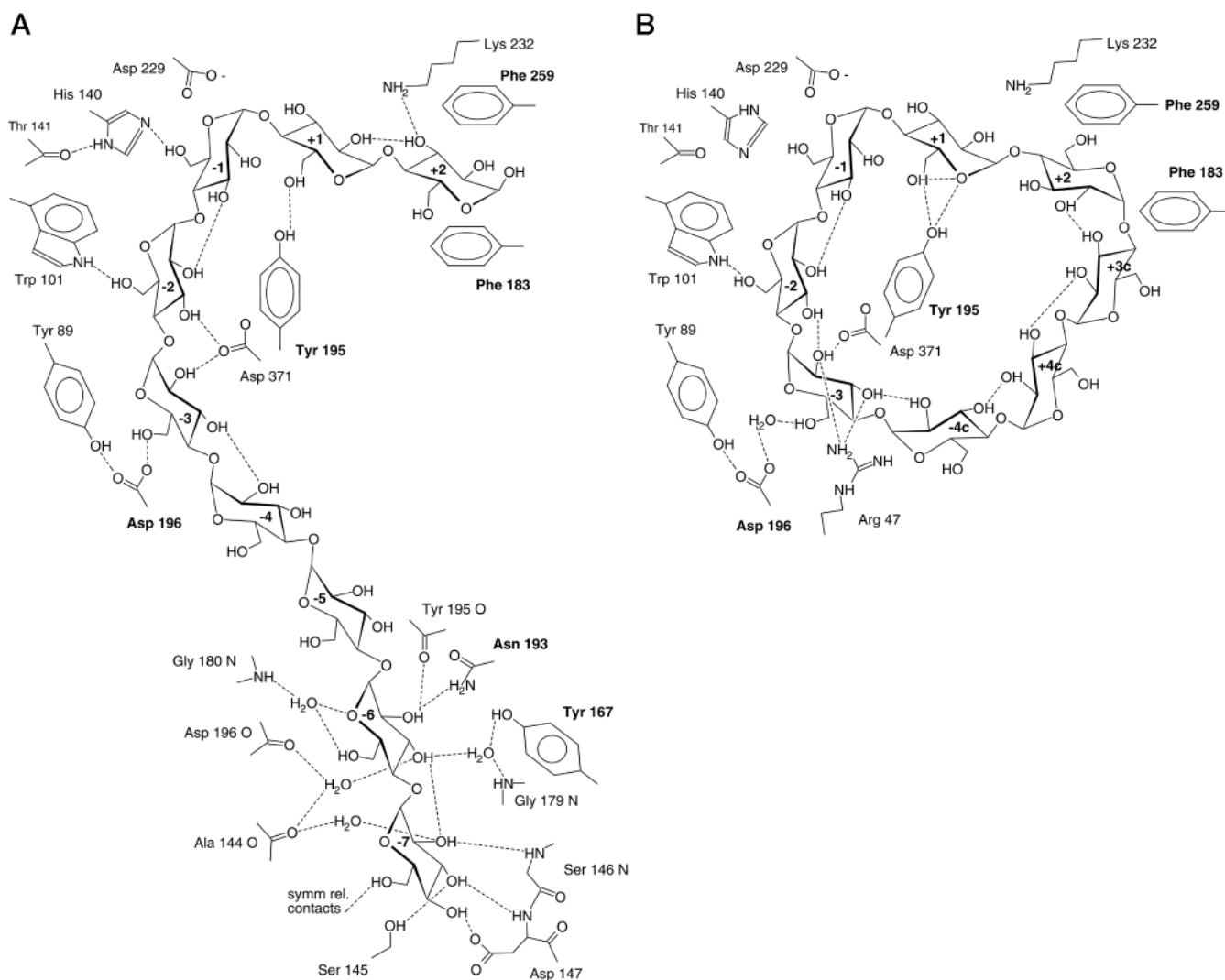
FIG. 5. **Overview of the interactions between CGTase and maltononaose (7) (A) or γ-cyclodextrin (B)**. The distances associated with the interactions are in Table III. For clarity, not all interactions at subsites −2, −1, and +1 are shown. *Symm rel. contacts*, contacts made to a symmetry-related CGTase molecule in the crystal.

conserved in CGTases, except for Arg-47, which is sometimes replaced by Lys or His. This conserved basicity might preserve a charge-charge interaction with Asp-371 (at ∼5 Å), which stabilizes the conformation of subsite −3. In addition, the non-conserved residues Tyr-89 and Asn-94 (at ∼5 Å from the sugar) are part of subsite −3, as shown by mutagenesis studies (Table I).

When the interactions of Arg-47, Tyr-89, Asp-196, or Asp-371 with carbohydrates are removed by site-directed mutagenesis, not only do the binding affinities (K_m) change for linear substrates or cyclodextrins, but a 4–10-fold decrease of the k_{cat} for cyclization and the reverse cyclodextrin degradation, or coupling, reaction results.[2,4] This indicates that, in addition to their role in substrate and product binding, residues at subsite −3 are actively involved in circularization. This important function of subsite −3 partly derives from its strategic position between the conserved subsites −1 and −2 (Table I) and the weakly binding subsites −4 and −5 (Table III). If the sugar orientation is changed at subsite −3, a large influence on the positions of sugars at more distant subsites is seen.

At Subsite +2 Phe-259 Stabilizes the Cyclodextrin Binding

Mode—In the later stages of circularization, the circular sugar chain reaches subsite +2, where it competes with free sugar acceptors (*e.g.* maltose) for binding. The x-ray structures indicate that Phe-183 and Lys-232 at subsite +2 preferably interact with such linear acceptors, which is consistent with the presence of homologous residues in α-amylases (Table I). Nevertheless, mutagenesis of Phe-183 indicates a critical role in cyclization (30). Possibly, Phe-183 is correctly positioned to guide the circularizing movement of the linear chain toward the acceptor sites. The x-ray structures further show that Phe-259 at subsite +2, a typical residue for CGTases, selectively stabilizes cyclodextrins. This is supported by mutants in Phe-259, which show a greater loss in affinity (as judged by the K_m value) for cyclodextrins than for maltose (30). Thus Phe-259 stimulates the use of a circularized sugar chain as the acceptor instead of a free sugar.

Conclusions—The active site of CGTase is an interesting example of an architecture in which a particular specificity is added to a conserved α-amylase bond cleavage machinery. Sequence comparisons (Table I) indicate that this bond cleavage machinery is located at subsites −2, −1, and +1, whereas the cyclization specificity is confined to subsites +2, −3, −6, and the centrally located residue Tyr-195. Our analysis of the structures of *B. circulans* strain 251 E257Q/D229N CGTase, in

complex with maltononaose and γ-cyclodextrin, confirms this picture. Maltononaose and γ-cyclodextrin are bound in similar ways at subsites -2, -1, and $+1$ but show conformational differences at subsites $+2$ and -3. At those latter subsites, specific "cyclodextrin binding" residues exist (Phe-259 and Arg-47) as well as "linear substrate binding" residues (Phe-183, Lys-232, and Asp-196). These separate functions can be exploited to engineer enzymes with specific properties. At subsite -6, the role of Asn-193 and Tyr-167 seems to be selecting a substrate of sufficient length for cyclodextrin formation (minimally 6 glucoses). Finally, the aromatic ring of Tyr-195 could bind an intermediary stage in circularization, since it is important for cyclization activity, but does not interact strongly with either linear substrate or cyclodextrin.

REFERENCES

1. Henrissat, B., and Davies, G. (1997) *Curr. Opin. Struct. Biol.* **7,** 637–644
2. Janeček, S. (1997) *Prog. Biophys. Mol. Biol.* **67,** 67–97
3. Svensson, B. (1994) *Plant Mol. Biol.* **25,** 141–157
4. Pedersen, S., Dijkhuizen, L., Dijkstra, B. W., Jensen, B. F., and Jørgensen, S. T. (1995) *Chemtech* 19–25
5. Crabb, W. D., and Mitchinson, C. (1997) *Trends Biotechnol.* **15,** 349–352
6. McCarter, J. D., and Withers, S. G. (1994) *Curr. Opin. Struct. Biol.* **4,** 885–892
7. Uitdehaag, J. C. M., Mosi, R., Kalk, K. H., van der Veen, B. A., Dijkhuizen, L., Withers, S. G., and Dijkstra, B. W. (1999) *Nat. Struct. Biol.* **6,** 432–436
8. Katsuya, Y., Mezaki, Y., Kubota, M., and Matsuura, Y. (1998) *J. Mol. Biol.* **281,** 885–897
9. Mukai, K., Tabuchi, A., Nakada, T., Shibuya, T., Chaen, H., Fukuda, S., Kurimoto, M., and Tsujisaka, Y. (1997) *Starch* **49,** 26–30
10. Klein, C., and Schulz, G. E. (1991) *J. Mol. Biol.* **217,** 737–750
11. Lawson, C. L., van Montfort, R., Strokopytov, B., Rozeboom, H. J., Kalk, K. H., de Vries, G. E., Penninga, D., Dijkhuizen, L., and Dijkstra, B. W. (1994) *J. Mol. Biol.* **236,** 590–600
12. Penninga, D., van der Veen, B. A., Knegtel, R. M. A., van Hijum, S. A. F. T., Rozeboom, H. J., Kalk, K. H., Dijkstra, B. W., and Dijkhuizen, L. (1996) *J. Biol. Chem.* **271,** 32777–32784
13. Strokopytov, B., Knegtel, R. M. A., Penninga, D., Rozeboom, H. J., Kalk, K. H., Dijkhuizen, L., and Dijkstra, B. W. (1996) *Biochemistry* **35,** 4241–4249
14. Schmidt, A. K., Cottaz, S., Driguez, H., and Schulz, G. E. (1998) *Biochemistry* **37,** 5909–5915
15. Knegtel, R. M. A., Strokopytov, B., Penninga, D., Faber, O. G., Rozeboom, H. J., Kalk, K. H., Dijkhuizen, L., and Dijkstra, B. W. (1995) *J. Biol. Chem.* **270,** 29256–29264
16. Strokopytov, B., Penninga, D., Rozeboom, H. J., Kalk, K. H., Dijkhuizen, L., and Dijkstra, B. W. (1995) *Biochemistry* **34,** 2234–2240
17. Wind, R. D., Uitdehaag, J. C. M., Buitelaar, R. M., Dijkstra, B. W., and Dijkhuizen, L. (1998) *J. Biol. Chem.* **273,** 5771–5779
18. Otwinowski, Z. (1993) in *Data Collection and Processing* (Sawyer, L., Isaacs, N., and Bailey, S., eds) pp. 56–62, SERC Daresbury Laboratory, Warrington, UK
19. Jones, T. A., Zou, J. Y., Cowan, S. W., and Kjeldgaard, M. (1991) *Acta Crystallogr. Sec. A* **47,** 110–119
20. Tronrud, D. E., Ten Eyck, L. F., and Matthews, B. W. (1987) *Acta Crystallogr. Sec. A* **43,** 489–501
21. Lamzin, V. S., and Wilson, K. S. (1993) *Acta Crystallogr. Sec. D* **49,** 129–147
22. Vellieux, F. M. D., and Dijkstra, B. W. (1997) *J. Appl. Crystallogr.* **30,** 396–399
23. Read, R. J. (1986) *Acta Crystallogr. Sec. A* **42,** 140–149
24. Harata, K. (1984) *Chem. Lett.* **241,** 641–644
25. Hooft, R. W. W., Vriend, G., Sander, C., and Abola, E. E. (1996) *Nature* **381,** 272–272
26. Collaborative Computational Project Number 4 (1994) *Acta Crystallogr. Sec. D* **50,** 760–763
27. Laskowski, R. A., MacArthur, M. W., Moss, D. S., and Thornton, J. M. (1993) *J. Appl. Crystallogr.* **26,** 283–291
28. Qian, M., Haser, R., Buisson, G., Duée, E., and Payan, F. (1994) *Biochemistry* **33,** 6284–6294
29. Brzozowski, A. M., and Davies, G. J. (1997) *Biochemistry* **36,** 10837–10845
30. Nakamura, A., Haga, K., and Yamane, K. (1994) *Biochemistry* **33,** 9929–9936
31. Koehler, J. E. H., Saenger, W., and van Gunsteren, W. F. (1988) *J. Mol. Biol.* **203,** 241–250
32. Hinrichs, W., Büttner, G., Steifa, M., Betzel, C., Zabel, V., Pfannemüller, B., and Saenger, W. (1987) *Science* **238,** 205–208
33. Brady, J. W., and Schmidt, R. K. (1993) *J. Phys. Chem.* **97,** 958–966
34. Vyas, N. K. (1991) *Curr. Opin. Struct. Biol.* **1,** 732–740
35. Steiner, T., and Saenger, W. (1994) *Carbohydr. Res.* **259,** 1–12
36. Nakamura, A., Haga, K., and Yamane, K. (1993) *Biochemistry* **32,** 6624–6631
37. Penninga, D., Strokopytov, B., Rozeboom, H. J., Lawson, C. L., Dijkstra, B. W., Bergsma, J., and Dijkhuizen, L. (1995) *Biochemistry* **34,** 3368–3376
38. Swift, H. J., Brady, L., Derewenda, Z. S., Dodson, E. J., Dodson, G. G., Turkenburg, J. P., and Wilkinson, A. J. (1991) *Acta Crystallogr. Sec. B* **47,** 535–544
39. Bender, H. (1985) *Carbohydr. Res.* **135,** 291–302
40. Bender, H. (1990) *Carbohydr. Res.* **206,** 257–267
41. Vetter, D., and Thorn, W. (1992) *Starch* **6,** 229–233
42. Tewari, Y. B., Goldberg, R. N., and Sato, M. (1997) *Carbohydr. Res.* **301,** 11–22
43. Meyer, J. E. W., and Schulz, G. E. (1997) *Protein Sci.* **6,** 1084–1091
44. Sin, K.-A., Nakamura, A., Masaki, H., Matsuura, Y., and Uozumi, T. (1994) *J. Biotechnol.* **32,** 283–288
45. Terada, Y., Yanase, M., Takata, H., Takaha, T., and Okada, S. (1997) *J. Biol. Chem.* **272,** 15729–15733
46. Fujiwara, S., Kakihara, H., Sakaguchi, K., and Imanaka, T. (1992) *J. Bacteriol.* **174,** 7478–7481
47. Parsiegla, G., Schmidt, A. K., and Schulz, G. E. (1998) *Eur. J. Biochem.* **255,** 710–717
48. Mattsson, P., Battchikova, N., Sippola, K., and Korpela, T. (1995) *Biochim. Biophys. Acta* **1247,** 97–103
49. Kim, Y. H., Bae, K. H., Kim, T. J., Park, K. H., Lee, H. S., and Byun, S. M. (1997) *Biochem. Mol. Biol. Int.* **41,** 227–234
50. Wind, R. D., Buitelaar, R. M., and Dijkhuizen, L. (1998) *Eur. J. Biochem.* **253,** 598–605